

# Effect of the Character of the (Ni, Pd) Cluster/Graphene Interatomic Bonds on the Thermosize Effects and Structural–Isomeric Transitions

V. A. Polukhin\*, E. D. Kurbanova, and A. E. Galashev

*Institute of Materials Science and Metallurgy of Ural Federal University, Yekaterinburg, Russia*

\**e-mail: pvalery@nm.ru*

Received January 12, 2012

**Abstract**—The thermal evolution of nanoclusters is studied by molecular dynamics simulation to analyze the nucleation and kinetics of the kinetic processes that determine the basic factors of the onset of premelting and the loss of thermal stability of a two-dimensional system of transition-metal (Pd, Ni) nanoclusters located on a graphene substrate. A comprehensive analysis reveals the effect of the initial structural characteristics of nanoclusters, the heating conditions, and the kinetic factors during thermally activated diffusion on the nanostructuring in the thermal evolution of the nanoclusters. This evolution includes the following stages: isomerization, quasi-melting, and the decomposition of a given regular structure; it is classified as an order–disorder transition and as an analog of phase transitions in macroscopic systems on the nanoscale.

**DOI:** 10.1134/S0036029512080083

## INTRODUCTION

The molecular dynamics (MD) simulation of the thermal stability of metallic nanoclusters with the optimum ratio of noncrystalline and crystalline coordinations (which correspond to the minimum cluster energy) in their structure is important for both a fundamental science and technological processes. An analysis of the results of this work and the revealed specific features of cluster structures promotes successful planning of real experiments to form new disperse materials with the required set of physicochemical, magnetic, and optical properties to design novel high-quality micro- and nanoelectronic devices in order to pass to the next level of miniaturization from the micro- to the nanorange. The application of nanocatalysts sharply increases the efficiency of catalytic hydrocracking, dewaxing of heavy oil fractions, hydroisomerization of gasoline fractions in the production of antiknock gasoline, hydropurification, hydrogenation, dehydration of methyl phenyl carbinol (based on Ni, Co, Mo, W nanoclusters), reforming, isomerization, and hydration (using nanoclusters of platinum group metals Pt, Ag, Ru, Pd).

An important problem of materials science in designing catalytic nanoclusters is to reveal the mechanisms of increasing the thermal stability of a nanostate and its substructural elements. It is necessary to retain the multilevel structure of the catalytic system of geometrically perfect internal coordinations and the surface of individual nanoclusters (2–3 nm) of transition metals (with four or five shells at an atomic diameter of 0.46 nm for Ni and 0.49 nm for Pd) and to

provide their precision positioning on a substrate in order to ensure an integral catalytic effect with controlled exchange of the charge states of clusters when a tunneling current appears between them. As follows from the experimental data in [1], the optimum number of atoms in transition-metal nanoparticles should not be larger than one thousand, which is also supported by the results of the MD simulation of icosahedral Pd<sub>561</sub> and Ni<sub>147–561</sub> nanoclusters performed in this work.

The most interesting fact in nanoscale catalysis is its efficiency as a result of a cooperative effect. In other words, catalytic activity is inherent in properly organized and spaced groups of clusters (2D spacers) rather than individual clusters (atoms in vertices and edges). These groups do not represent the joining of catalytically active reagents into a general macroscopic system with a fixing surface in the classical scheme of chemical catalysis.

The unique catalytic, magnetic, and optoelectronic properties of nanoclusters are based on not only the organization of internal coordinations and surface parameter but also on their cooperative self-organization as 2D spacers on substrates and as 3D spacers in solutions or skeleton constructions. Electronic nanocluster restructuring events in both the internal structure of individual clusters and cooperative self-organization proceed in several picoseconds and cannot always be detected by modern measuring equipment. It is these space–time scales that are characteristic of very important thermally activated nanoprocesses in the presence of various quantum effects. For example,

the effect of a significant decrease in the electron free path length because of specular reflections along one or all dimensions of a nanosystem (quantum well or dot, respectively) is one of them.

However, the maximum catalytic activity of clusters of some metals (e.g., Pt) is achieved when atoms are located in highly coordinated positions on faces, and a high density of edges on a cluster surface creates an additional barrier to the kinetics of reaction fragments. The interaction of nanoparticles with the material forming a fixation surface, which is not inert in the general case, is also important in nanoscale catalysis. Apart from enhancing a cooperative catalytic effect, a substrate substantially increases the thermal stability of clusters, preventing intense leaching (i.e., atomic emission into a reactive zone). When choosing a substrate, one can enhance the interaction between cluster atoms and the substrate and control the thermal stability of the cluster, increasing its melting temperature.

The purpose of this work is to perform MD simulation of the thermal evolution of nanoclusters and the nucleation and activation of the kinetic processes that determine the basic factors of premelting and the loss of thermal stability of the main element of catalytic interactions, namely, a two-dimensional system of transition-metal (Pd, Ni) nanoclusters located on a graphene substrate. One of the basic problems to be solved is to find physicochemical conditions and factors for enhancing the thermal stability of clusters with different symmetries of their coordinations during the formation of crystalline (fcc, hcp, bcc) and noncrystalline (odd and fractional symmetry) structures of transition-metal clusters Pd<sub>N</sub> and Ni<sub>N</sub> containing  $N = 13$ –561 atoms at given sizes and shapes.

As a result of a comprehensive analysis, we found the effect of the initial structural characteristics, the heating conditions, and the kinetic factors during thermally activated diffusion on the controlled structuring of nanoclusters during their thermal evolution. This process includes the following stages: isomerization; “quasi-melting”; and fracture of a given regular structure, which is classified as an order–disorder transition. On the nanoscale, this transition is a certain analog of a phase transition in macroscopic systems [1–4].

Using computer simulation and physically grounded interatomic interaction potentials, we [5–7] were able to reveal the basic laws of the nucleation and growth of nanoclusters, the sequential and defectless formation of coordination shells, structural–isomeric transitions, the morphological features of cluster surfaces, and the physicochemical parameters required to obtain functional nanoclusters on an atomic–molecular scale.

## INTERATOMIC INTERACTION POTENTIALS

In the available database of various versions of computer simulation, the interatomic interaction potentials are calculated using various approximations, which differ in the complexity and accuracy of taking into account multiparticle effects. Therefore, when choosing techniques for transition metals, we took into account the specific features of clusters to be simulated, the presence of an open surface, the regularity of the cluster, and the interaction with an immobilizing substrate. To this end, we analyzed the available multiparticle interaction potential of transition-metal atoms (Pd<sub>N</sub>, Ni<sub>N</sub>) in the case of isolated clusters located on a substrate in contact with other phases. After testing calculations for estimating the binding energies, we chose the Sutton–Chen multiparticle potential [8] for Ni clusters,

$$E = \varepsilon \left[ 1/2 \sum_i \sum_{j>i} V_{\text{omm}}(R_{ij}) - C \sum_i (\rho_i)^{1/2} \right]. \quad (1)$$

where  $\varepsilon = 15.7071 \times 10^{-3}$  eV for Ni;  $C = 39.432$ ,  $\rho_i = \sum (a/r_{ij})^m$ ;  $V_{\text{omm}} = (a/r_{ij})^n$ ;  $a$  is the equilibrium lattice parameter; and power integer parameters  $m$  and  $n$  for Ni are 6 and 9, respectively.

For Pd, we used the Cleri–Rosato tight-binding potential (TBS) [9],

$$E_{cl} = \sum_i (E_b^i + E_r^i), \quad (2)$$

where  $E_b^i$  is the contribution of the  $i$ th atom created by multiparticle attraction and  $E_r^i$  is the contribution of the Born–Mayer repulsive interaction for the  $i$ th atom.

Contributions  $E_b^i$  and  $E_r^i$  are

$$E_b^i = \left\{ \sum_{j, r_{ij} < r_c} \xi^2 \exp \left[ -\frac{q}{\alpha} \left( \frac{r_{ij}}{r_0} - 1 \right) \right] \right\}^\alpha, \quad (3)$$

$$E_r^i = \sum_{j, r_{ij} < r_c} A \exp \left[ -p \left( \frac{r_{ij}}{r_0} - 1 \right) \right]. \quad (4)$$

Free parameters  $A$ ,  $\xi$ ,  $p$ ,  $q$ , and  $r_0$  of the TB–SMA potential are adjusted from the experimental values of the binding energy, the lattice parameter, and the independent elastic constants of pure metals and alloys. The parameters of potentials (3) and (4) are given in the table. In Eq. (4),  $r_c$  is the interaction cutoff radius.

To simulate metal–carbon systems in estimating  $M$ – $C$  interatomic interactions, we used various combinations on the basis of exponential Morse-type potentials [10]

$$V(r_{ij}) = \sum_{j>1} E_{\text{PdC}} [\exp(-2\kappa[r_{ij} - r_{\text{PdC}}])]. \quad (5)$$

Tight-binding (TB) potentials for the atomic interaction in a  $\text{Pd}_N$  cluster and the interaction of  $M$  with carbon in the interface layer of a heterostructure

| TB potential |         | Morse                  |        |
|--------------|---------|------------------------|--------|
| Parameters   | Pd      | Parameters             | Pd–C   |
| $A$ , eV     | 0.1746  | $E_{\text{PdC}}$ , eV  | 0.1132 |
| $\xi$ , eV   | 1.718   | $r_{\text{PdC}}$ , nm  | 0.273  |
| $p$          | 10.867  | $k$ , $\text{nm}^{-1}$ | 15.56  |
| $q$          | 3.742   |                        |        |
| $r_0$ , nm   | 0.27485 |                        |        |

### RESULTS OF THE MD SIMULATION OF ISOLATED (UNATTACHED OR FREE) NANOCCLUSERS

The temperature-dependent rate of filling of faces with atoms is an important factor that determines the nanocluster (crystallite) shape in real cluster formation processes. Based on the temperature range under study, the kinetic energy of joined atoms (fragments), and the barrier spectrum, we determine the growth kinetics, the details of joining, the geometrical laws of structure formation, and the deviation from the regular configurations of formed clusters for joining events. Information on all factors affecting the cluster growth and shape is presented for some substances in the form of Nakaya diagrams [2]. The process of shaping can be efficiently controlled using surfactants, which affect the adsorption kinetics, supersaturation, joining acts, the chemical activity of aggregation with the formation of spheroid polyhedra, and their coherent (along joined coordinations) hybridization.

With an MD simulation, we studied the thermal evolution (during steplike heating from 300 to 1500 K at a step of 50 K) of perfect transition-metal nanoclusters  $\text{Ni}_N$  and  $\text{Pd}_N$  containing 13–561 atoms and having various initial structures (fcc, bcc, Ih). As follows from the results of MD simulation, the melting of  $\text{Ni}_{309}$  and  $\text{Ni}_{569}$  clusters occurs within a significant temperature range, in contrast to the melting of macroscopic bodies. This range contains the stage of quasi-melting,

where a solidlike state is also present (e.g., for a cluster consisting of 4 shells and 309 atoms, 55 atoms in central shells are in the solidlike state and 254 atoms are in the fluid state). Upon subsequent heating, an Ih (icosahedral) structure of clusters containing up to  $10^3$  atoms becomes energetically stable, which is illustrated in Fig. 1 (atomic projections onto the  $XY$  plane) reflecting structural transformations. For clarity of diffusion, half of the circles representing atoms is white and the other half is black. Figure 2 shows the changes in the potential energy that characterize the energetics of structural transformations. Depending on the number of atoms in clusters, the temperature ranges of cluster melting were detected from a change in the potential energy: from the boundaries of the beginning and end of a smooth steplike increase in a curve upon heating from 300 to 1500 K; e.g., the temperature ranges of melting for  $\text{Ni}_N$  and  $\text{Pd}_N$  are 200–300 and 650–870 K at  $N = 55$  and 561, respectively.

When simulating heating of fcc Ni and Pd nanoclusters, we revealed specific thermosize effects of atomic coordinations, namely, the loss of structural stability induced by the isomeric transformation of fcc cuboctahedra into icosahedra. By analogy with macroscopic bodies, the melting of clusters with a perfect polyhedral structure begins with their surface, and it is initiated by the displacements of the atoms located at vertices and edges and, then, the neighboring atoms on external shell faces. In this case, the atoms in the inter-

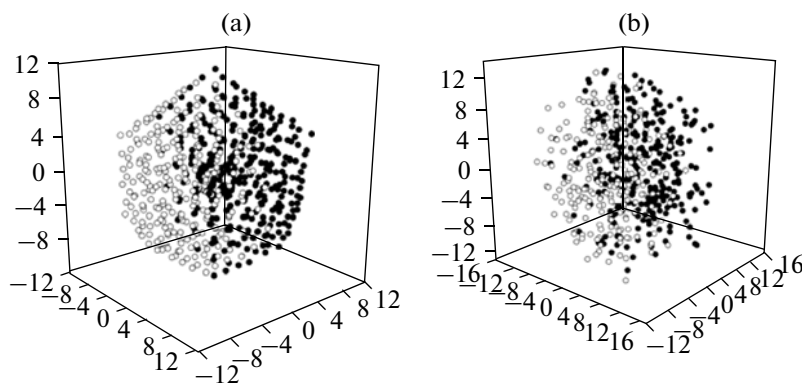


Fig. 1.  $\text{Ni}_{561}$  nanoclusters with an initial Ih structure at (a) 300 and (b) 1500 K (atomic coordinates are given in nm).

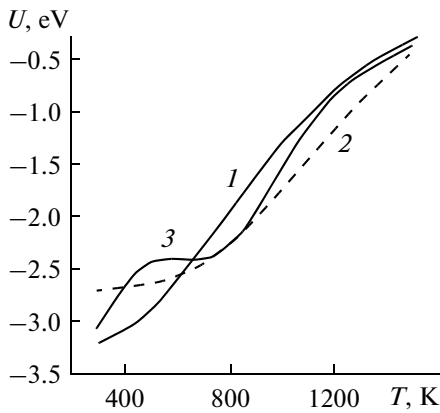


Fig. 2. Temperature dependence of the potential energy of  $Ni_{561}$ : (1) fcc, (2) bcc, and (3) Ih.

nal shells (center) are rigidly fixed at their vibration sites.

At the next stage (quasi-melting), the phase transition (melting) ends in sequential transition of all shells beginning from the surface (first, a faceted structure and, then, a shell structure of a cluster disappears) into a fluid state. This development of diffusion processes takes place in nanoclusters, since their volume has no defects such as vacancies, dislocations, disclinations, and developed grain-boundary surface, which are inherent in real polycrystalline metals. An increase in the fraction of surface atoms in the nanosize limit does determine the diffusion mobility mechanisms caused by the cluster surface morphology. The functional properties of clusters are determined by their geometry and shape, i.e., the absence of adsorbed (external) and self-adatoms, which are always present on the surface of bulk crystals at ordinary temperatures and determine surface diffusion mechanisms. However, for these mechanisms to operate in a cluster, it is necessary to create thermal conditions for some atoms in the near-surface layers to become adatoms capable of surface migration. Therefore, a certain activation energy is necessary for a surface-coordinated atom to transform into an adatom with the minimum energy consumption. The atoms on the vertices and edges of a cluster ( $N_0$ ) are the best candidates for this thermally activated transformation. Assuming that heating of a cluster to temperature  $T$  leads to the appearance of  $N_a$  adatoms, we can describe the mechanism of this activation by the exponent  $N_a = N_0 \exp(-E/k_B T)$ .

For example, the thermosize effects manifest themselves in a substantial decrease in the melting temperature of clusters, which is visible in the caloric curves in Fig. 2.

Hence, the diffusion in nanoclusters in heating is initiated by activated tangential displacements on a surface and the appearance of pair structural defects, namely, the vertex atoms rejected to the surface and

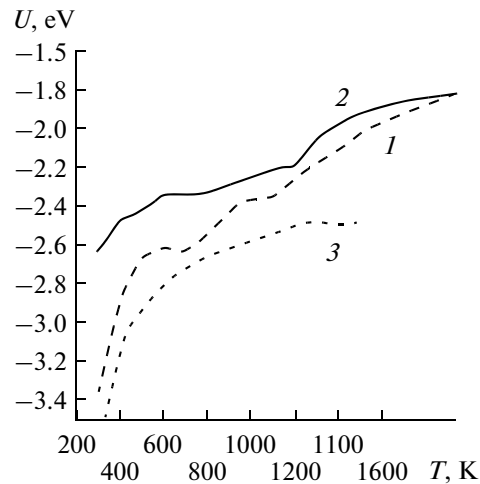
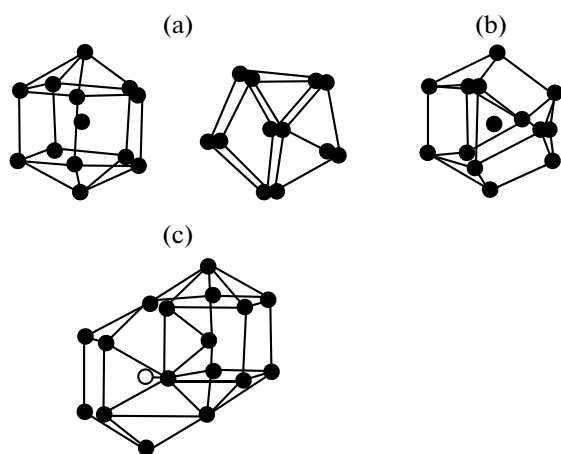


Fig. 3. Temperature dependence of potential energy  $U(T)$  for nickel nanoclusters with various initial structures. Heating of isolated clusters: (1) fcc  $Ni_{309}$ , (2) vitrification of  $Ni_{309}$  melt, and (3) Ih  $Ni_{561}$ .

classified as “adatoms” and the vacancies that form and drift in the surface shell along edges.

Thus, diffusion first develops via atom exchange on edges and, then (upon heating), via exchange between the neighboring atoms on faces. However, when heating is terminated, the drift of a vacancy as a void can end in its deformation between two coordination sites (vacancy “splitting” effect). When the diffusion process develops deep into a cluster, the stability of vacancies increases from the periphery to the center of the cluster as a result of enhanced correlated displacements during an exchange diffusion mechanism. The subsequent appearance of adatoms due to the rejection of atoms from the surface shell can occur due to heat supply or a strong kinetic energy fluctuation. The nanosize effects in clusters, which represent small objects with strong density fluctuations, begin to manifest themselves before melting as structural–isomeric transitions with a continuous process of coordination transformations (i.e., isomerization) during a continuous redistribution of the kinetic and potential energies. They manifest themselves as specific thermosize effects, i.e., the loss of structural stability initiated by the isomeric transformation of fcc cuboctahedra into icosahedra.

It is difficult to study the growth of a solidifying phase from molten clusters because of the limiting size of the cluster model and the nucleation time. Therefore, we study ultrarapid quenching with the formation of metastable states, namely, amorphous and partly disordered states with predominant icosahedral coordinations (Fig. 3). During slower cooling, various versions of structure formation between octa-, cuboctahedron, amorphous, icosahedral, quasicrystalline, and other dynamic hybrid forms (i.e., bifurcations) can take place [1, 17, 18]. The structural changes dur-



**Fig. 4.** Top row: (a) Ino decahedron and (b) hcp lattice coordination polyhedron. Bottom: (c) combined Ino and hcp polyhedra.

ing rapid cooling are irreversible, and an amorphous structure is retained with the formation of a high-energy glassy cluster at 300 K.

In the case of Ni clusters, a solidlike configuration with regular bcc or Ih coordinations and a significantly lower fcc probability forms only during very slow cooling of a drop. For a comparison of the nanostructuring processes in palladium and nickel, Fig. 4 shows the most stable Pd clusters (Figs. 4a, 4b) and a coherent Ni cluster (Fig. 4c) that were found by a statistical–geometric analysis. Thus, in contrast to Pd<sub>561</sub> clusters [16], Ni<sub>561</sub> nanoclusters are characterized by the presence of hybrid Ino decahedra (Dh) [17], which combine a crystalline structure in the presence of five square faces and fivefold axial symmetry. (The fivefold axis in the Ino decahedron connects the two vertices of the opposite bipyramids, and this decahedron contains directions the angles between which (109°) coincide with those for the hcp coordinations with an axial ratio  $c/a = 1.633$ .)

Note that the thermosize effects manifest themselves in not only the temperature dependences of the characteristics that are controlled during the MD simulation (pressure, internal stress) but also in anomalous behavior of heat capacity. The melting of nanoclusters covers a wide temperature range and proceeds during the coexistence of fluid- and solidlike states, which represent quasi-melting that finishes the melting phase transition: further heating results in melting with structural homogenization of a melt, and cooling can lead to the restoration of the initial situation.

#### THERMOSIZE EFFECTS OF A SUBSTRATE

It should be noted that, apart from influencing the general topology of the surface and internal structure, an electron-charge state and a substrate determine the

self-organization of clusters by taking part in their cooperative interaction and the redistribution of the electron density, which eventually affects the catalytic efficiency. The maximum activity of nanoclusters was found to be related to a sharp increase in the electrical conductivity of the immobilizing material and to its semiconductor properties having acquired upon the redistribution of the electron density over the entire catalytic ensemble made of metallic nanoparticles and an immobilizer. This charge redistribution enhances the catalytic activity only at a certain optimum number of atoms in each nanocluster and does not exert the required effect when a charge is delocalized in large clusters. In this case, the participation of the material of a fixing matrix in a charge redistribution is not necessary if metal nanoclusters are sufficiently close for temperature-activated charging or the fluctuation electrical transfer between catalyst particles. Apart from the nanoscale parameters of the clusters, we should speak about the second type of three-dimensional clusters, namely, the nanocluster spacing corresponding to thermodynamic conditions. Along with coherent crystalline fragments, a cluster nanophase can be represented by structures with noncrystalline symmetry, such as dodecahedral or icosahedral, or by an aperiodic (incommensurably modulated) structure with cubic symmetry [1, 17], which were identified for systems with equilibrium and complex metastable structures.

The thermal stability of clusters depends on both their internal structure and the interaction with fixing substrates (immobilizers) along adjoining faces. Carbon nanotubes, graphene planes, metal nitrides, and silicon and metal oxides (e.g., TiO<sub>2</sub>) are promising materials for such substrates [18, 19]. Even the first experiments demonstrated a high activity, selectivity, and thermal stability of catalysts made of palladium nanoclusters located in nanotubes and on graphene planes during the hydrogenation of some important reagents as compared to traditional catalysts [1, 17]. To increase the catalyst efficiency, it is necessary to search for and select a specific inert material for fixing substrates apart from achieving a high thermal stability of a cluster structure, a high density at vertices and edges (i.e., active centers), an increase in the total area of a highly developed contact surface made of regularly and properly spaced clusters, and a retained initial cluster configuration. The contact of metallic clusters with metals results in a thermoelectric potential accompanied by electron transfer to a metal with a lower Fermi energy. In contact with an insulator, metallic clusters are easily polarized and cause the related polarization in the insulator, which leads to a fixing effect.

Using MD simulation, we analyzed the results obtained with allowance for the thermal evolution of clusters during their fixation on a substrate (Fig. 5) [18–20]. As the material of a fixing substrate or a shell–capsule in MD models, we chose silicon oxide,

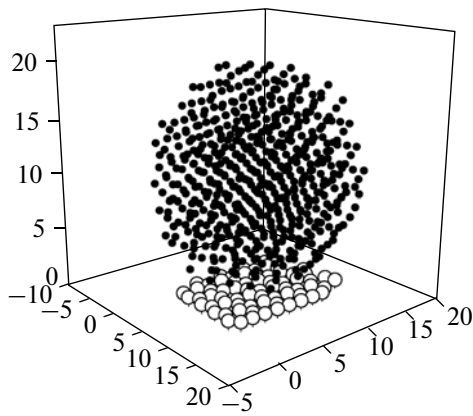


**Fig. 5.** Pd<sub>561</sub> nanocluster with an initial Ih structure on a graphene substrate at  $T = 1300$  K (atomic coordinates are given in nm).

copper nitride, or diamond. The interaction of metal cluster atoms with substrate atoms for the metal–carbon and metal–silicon oxide systems was described in test calculations using combined potentials and the Ruffi-Tabar method with the Morse or Lennard–Jones potentials and the parameters estimated in [10]. We chose combined Morse potentials, since they most precisely described the results of quantum-mechanical calculations upon parametrization [21].

Clusters with {111} faces in an initial icosahedral structure or with the unstable faces having appeared after isomerization and transformation ({100} and {110}) were found to be most resistant to heating. The contours of the faceted morphology of clusters remained the same and smeared up to complete melting of all shells in spite of fluidization as a result of the heating-initiated diffusion motion of atoms in the surface shell.

Both the cluster melting kinetics and the heating thermodynamics change substantially under the action of a substrate. The temperature dependence of the phonon contribution to specific heat  $C_V$  was found to change upon heating and melting of a nanocluster. This contribution can be estimated by the integration of the vibration frequency spectrum of  $\omega$  atoms in a cluster  $D(\omega)$  from 0 to  $\infty$  as the Fourier transform of autocorrelation velocity functions  $v_i(t_0 + n\Delta t)$  [1]. The electron component of the contribution is determined in terms of the density of states at the Fermi level  $N(E_F)$  [18] and also depends on temperature,

$$C_e = \pi^2 k_B^2 T N(E_F) / 3. \quad (6)$$

Note that the self-diffusion coefficient can be estimated through the frequency spectrum at  $\omega = 0$ . However, the estimation of diffusion in terms of the root-mean-square displacement is mainly used in MD experiments. Specific heat  $C_V$  is estimated in terms of the root-mean-square fluctuations of kinetic energy

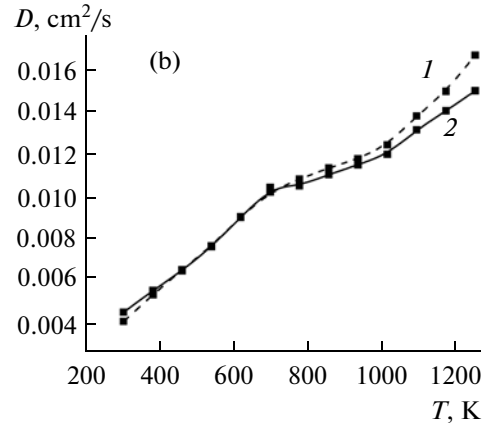
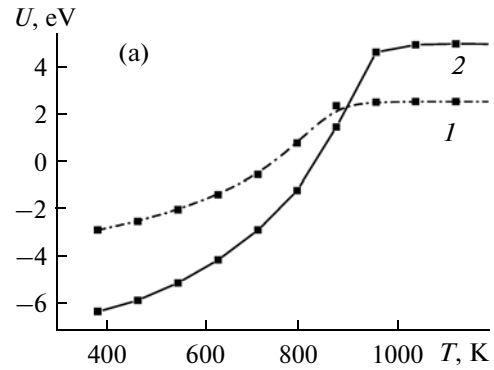


**Fig. 6.** Temperature dependences of (a) potential energy of Pd<sub>561</sub> nanoclusters and (b) diffusion coefficient. Heating of (1) isolated cluster and (2) cluster on a graphene substrate.

(as temperature fluctuations) or internal (potential  $U$ ) energy,

$$C_V = (\langle U^2 \rangle - \langle U \rangle^2) / Nk_B T^2, \quad (7)$$

where  $N$  is the number of atoms in the cluster.

The temperature-induced changes in the thermodynamic characteristics such as the internal energy (caloric curve for potential energy  $U(T)/N$  per atom) and the specific heat are also illustrative for the manifestation of the thermosize effects and the effect of a substrate (Figs. 6, 7). It should be noted that the non-monotonic temperature dependence of the caloric curve mainly reflects complex structural transformation processes and the modification of cluster states rather than a gradual decrease in, e.g., the shear moduli. The energy redistribution with increasing surface contribution  $\Delta G_s$  and decreasing internal contribution  $\Delta G = \Delta G_{in} + \Delta G_s$  results in nonadditive thermodynamic components as the manifestation of the thermosize effect, which is most pronounced in the temperature dependence of specific heat  $C_V$  calculated by Eq. (6) during the MD simulation of isolated palladium nanocluster Pd<sub>561</sub> upon heating from 300 to 1500 K. At the first stage of heating, the change in the specific heat  $C_V = T(dE/dT)_V \{ C_p = T(dE/dT)_p +$

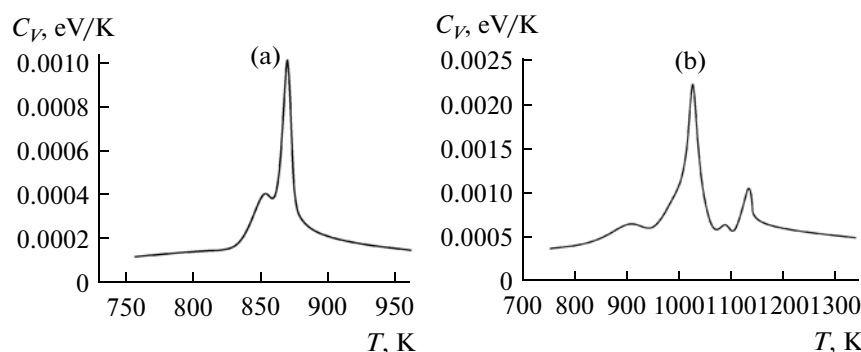


**Fig. 7.** Temperature dependences of specific heat  $C_V$  of (a) free  $\text{Pd}_{561}$  nanocluster and (b)  $\text{Pd}_{561}$  nanocluster on a graphene substrate upon heating from 300 to 1200 K.

$(3R/2)\delta(E)\}$ , which is also determined statistically at a constant pressure as  $C = [\langle E^2 \rangle - \langle E \rangle^2]/(k_B T^2)$  (where  $E$  is the total energy), is extremely nonuniform, almost anomalous.

We estimated the effect of substrate (carbon) atoms only to calculate the deformation of the atomic coordinations in the next shells. This effect is considered to be substantial only in the zone of heating and the appearance of nonzero tangential diffusion, which causes strong distortions in the coordinations in the contact zone and results in leaching due to the adsorption of some cluster atoms by the surface. The fixation of more than 10% of the cluster surface atoms in the contact zone strongly affects the heating dynamics and increases the melting temperature. The strong bonds in the contact zone also affect the atoms in the next layers. The balance between the momenta of neighboring shells changes substantially, and the rate of “mutual slip” of atoms in neighboring shells decreases. Further heating enhances the role of the substrate up to the “slump” of a spheroid and a noticeable broadening of an adhesion zone, leading to the retardation of an additional part of atoms and the rejection of them from an active exchange diffusion process.

It should be noted that the investigation of the effect of a substrate on the electron-charge distribution on a cluster surface (including long-range profile of near-surface electron density  $\rho(R)$  and  $k_F = 2\pi/\lambda$ ) and the conditions of appearance of a tunneling current in a system of spaced ( $1 \text{ nm} \sim d = \lambda/2$ ) 2D spacers requires other quantum-statistical methods for estimating electron states [18–22]. It is the retained state of charging that results in the drift of the nanoparticles located on a substrate with respect to each other so that they become equidistant and uniformly distributed in a hexagonal structure.

A substrate activates restructuring, which manifests itself in decreasing the melting and solidification ranges. Moreover, the structure of  $\text{Pd}_{561}$  nanoclusters during solidification did not correspond to the fcc structure of isolated nanoclusters and bulk samples. At

various stages of heating and solidification, this structure was represented by Ih and hcp coordinations on the nanoscale [16, 17]. The formed coordinations turned out to correspond to none of those characteristic of isolated clusters with the maximum possible bond density: an fcc rather than an icosahedral structure was found to be energetically stable for  $\text{Ni}_{561}$  on a substrate. The stabilizing ability of the substrate is illustrated by comparing the diffusion coefficient upon heating of free nanoclusters and nanoclusters on a graphene substrate (Fig. 6b). The temperature-induced changes in the onset of polymerization and melting and the temperature dependence of the internal energy (caloric curve for potential energy  $U(T)/N$ ) of isolated clusters and clusters on a graphene substrate are also illustrative for the manifestation of the thermosize effects and the effect of a substrate (Fig. 6a).

The interaction of a cluster with a substrate was found to affect the recoordination of metal atoms in the interface layer of a formed heterostructure and the heating thermodynamics and the melting kinetics of clusters. This behavior is reflected in the temperature dependence of the phonon contributions to specific heat  $C_V$  in heating and melting of Pd nanoclusters on a graphene substrate (Fig. 7).

The thermally activated effect of a substrate and the appearance of nonzero tangential diffusion result in both strong distortions of the metal atom coordinations in the contact zone and the leaching effect due to the adsorption of individual cluster atoms by the substrate surface.

For example, the atoms in  $\text{Pd}_N$  and  $\text{Ni}_N$  ( $N = 309, 561$ ) clusters located on graphene substrates interact with carbon at 370–420 K and form hexagons from carbon atoms with single and binary bent  $sp^2$  and  $sp^3$  bonds, i.e., ring clusters, in the (111) face/graphene contact zone (Fig. 8). The motion of metal and graphene atoms toward each other can be explained by their increasing attraction due to the overlapping of the  $d_z$  orbitals of the transition-metal and the  $\pi$  atoms of the graphene substrate [20–25].

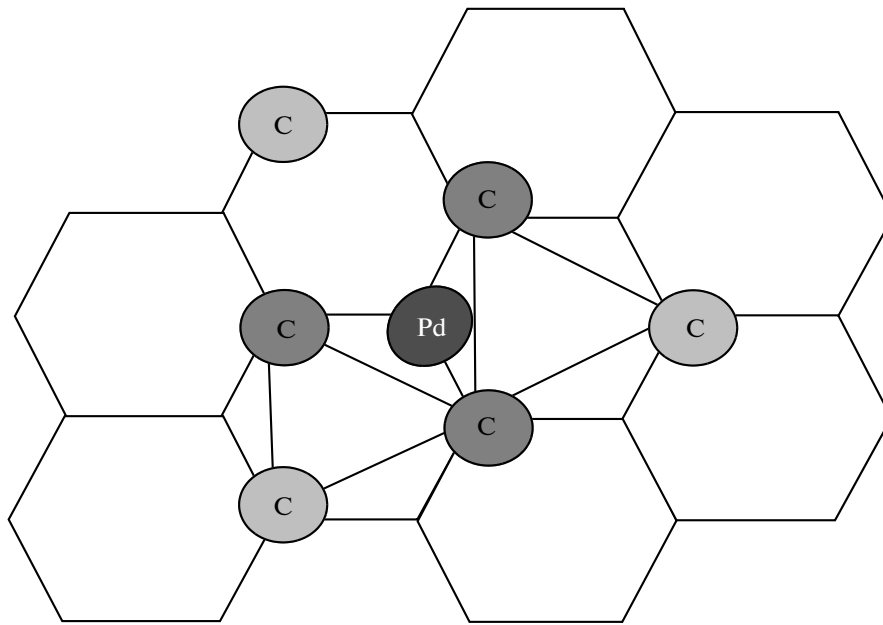


**Fig. 8.** Formation of the heterostructure of the  $\text{Pd}_{561}/\text{G1}$  interface through the formation of  $\text{Pd}_1\text{C}_6$  ring clusters as an analog of premelting isomerization.

## CONCLUSIONS

When analyzing the results of a computer simulation of the thermal evolution of isolated and fixed (on a graphene substrate) transition-metal (Pd, Ni) nanoclusters, we revealed the specific features of melting nucleation and activation that determine the main factors of an increase in the thermal stability, the isomerization temperature, the quasi-melting temperature, and the temperature of full melting of clusters. It was found that the beginning of thermodynamically activated diffusion is related to the appearance of adatom and vacancy pairs as a result of the displacement of vertex atoms from their sites and their subsequent migration during position exchange with the nearest atoms located on edges and, upon further heating, with the atoms of the adjacent faces. The temperature ranges of all heating stages, namely, structural isomerization and the coexistence of fluidized shells and solidlike central shells, correlate with not only the given structure and the number of nanocluster atoms but also with the interatomic interactions of cluster atoms with the substrate and depend on the geometry of the cluster faces in contact with the graphene plane. We also determined the minimum sizes of Pd and Ni nanoclusters ( $21d-23d$ , where  $d$  is the Pd or Ni atom diameter) at which an initial fcc structure can be retained as the most stable structure required for a number of devices with given temperature–time operating conditions (working temperatures).

It is also important that we revealed melting–solidification hystereses for  $\text{Pd}_N$  and  $\text{Ni}_N$  clusters with various initial structures and numbers of atoms and the limiting temperatures of stability loss (beginning of isomerization) for initial regular modifications as a

function of the cluster size. Moreover, we determined the temperature–time conditions for the formation of regular coordinations (fcc, hcp, Ih) during solidification and estimated their statistical weights and the stability ranges. The fraction of the structure consisting mainly of icosahedral coordinations and a low content of the Ino coordinations [17] increases in a certain range as the cooling rate increases. Outside this range, an amorphous structure with a gradual decrease in more stable residual Ino coordinations, as a hybrid of even and odd symmetries, becomes more competitive. A substrate was found to affect the specific heat: an additional structure, which is caused by the  $sp^2 \rightarrow sp^3$  rehybridization and the formation of new moire pattern coordinations in a growing contact zone, appears behind the principal peak in specific heat curves  $C_V(T)$  when a cluster on graphene is heated.

Thus, before a real experiment, the developed simulation program makes it possible to perform high-accuracy calculations of the required parameters of functional devices, mainly catalytic 2D spacer systems based on perfect clusters of other transition metals, at adequately chosen interatomic interaction potentials. The “melting” of  $\text{Pd}_N$  and  $\text{Ni}_N$  clusters was shown to occur as a transition from a regular to a disordered structure with a high atom migration mobility rather than as phase transitions. This transition has a more complex mechanism compared to the melting of macroscopic crystals, since it

(i) takes place in a wider temperature range (about one-third of the heating range) and

(ii) proceeds in several stages, namely, isomerization, quasi-melting, and the disappearance of a faceted morphology and a shell structure.

Of course, the study of the properties of clusters is important for materials science in designing cluster catalysts, optoelectronic devices, and magnetic storage media. The reliability of operation under various operating conditions is one of the most important characteristics of such devices, which is related to the stability of the working characteristics of cluster materials, mainly at elevated temperatures.

## REFERENCES

1. V. A. Polukhin and N. A. Vatolin, *Simulation of Disordered and Nanostructured Phases* (UrO RAN, Yekaterinburg, 2011).
2. E. Roduner, *Size Effects in Nanomaterials* (Tekhnosfera, Moscow, 2010).
3. V. A. Polukhin, E. D. Kurbanova, and A. E. Galashev, "Structural–Isomeric Changes and Stability of Nanocluster States of Nickel According to MD Simulation Data," in *Proceedings of Russian Conference on Physical Properties of Metals and Alloys, Yekaterinburg* (UGTU–UPI, Yekaterinburg, 2009), pp. 3–6.
4. V. A. Polukhin, E. D. Kurbanova, L. K. Rigmant, et al., "Molecular Dynamics Simulation of the Size Effects and the Thermal Stability of *d*-Metal (Ni, Pd) and Silicon Nanoclusters," *Perspektivnye Materialy*, No. 4, 13–21 (2009).
5. E. D. Kurbanova, L. K. Rigmant, and V. A. Polukhin, "Comparative Analysis on Heating- and Melting-Induced Changes in the Physicochemical Properties of Silicon and Nickel Nanoclusters," *Vestnik Kazanskogo Tekhnol. Univ.*, No. 1, 75–79 (2010).
6. a. V. A. Polukhin, E. D. Kurbanova, and A. E. Galashev, "Thermosize Effects, Isomerization, and Stability of Catalytic  $M_{147-561}$  Nanoclusters (2D Spaceps) of Transition Metals," *Vestnik Kazanskogo Tekhnol. Univ.*, No. 1, 92–96 (2010).
6. b. V. A. Polukhin, A. E. Galashev, and E. D. Kurbanova, "Increasing the Thermal Stability of Silicon, Nickel, and Palladium Clusters by Nanostructuring: Assemblers, Intercalates, and Hydrides. MD Experiment," in *Proceedings of V International Conference on New Promising Materials and the Process of Their Production, Volgograd* (IUNL VolgGTU, Volgograd, 2010), pp. 63–66.
7. V. A. Polukhin, E. D. Kurbanova, and L. K. Rigmant, "Nanoclusters—Intermediate State of Matter: Atomic Composition—Clusters—Alloy Phases. MD Simulation of Ni, Pd, and Fe Clusters," in *Proceedings of 10th Russian Seminar on Computer Simulation of the Physicochemical Properties of Glasses and Melts, Kurgan* (Kurgan. Gos. Univ., Kurgan, 2010), pp. 12–13.
8. A. P. Sutton and J. Chen, "Long-Range Finnis Sinclair Potentials," *Phil. Mag. Lett.* **B 9** (1), 139–143 (1990).
9. F. Cleri and V. Rosato, "Tight-Binding Potentials for Transition Metals and Alloys," *Phys. Rev. B* **48** (1), 22–33 (1993).
10. G. A. Mansuri, *Principles of Nanotechnology* (Nauchnyi Mir, Moscow, 2008).
11. V. A. Polukhin, E. D. Kurbanova, and L. K. Rigmant, "Thermal Stability of Catalytic Nanoclusters  $TM_{147-561}$ : Ni, Pd (2D Spacers)," *Butlerovskie Soobshcheniya* **25** (7), 1–12 (2011).
12. V. A. Polukhin and E. D. Kurbanova, "Structural Transformations during the Thermal Evolution of Metal (Ni, Pd) Nanoclusters under the Effect of a Substrate. MD Simulation," in *Proceedings of International Conference on Modern Metallic Materials and Technologies (SMMT-2011), St. Petersburg* (Politekh. Univ., St. Petersburg, 2011), pp. 262–264.
13. V. A. Polukhin, E. D. Kurbanova, and A. E. Galashev, "Comparative Analysis of Thermoscale Effects, Isomerization and Stability of TM–Nanoclusters (Pd, Ni, Fe) and Si in Dependence on Interatomic Potentials. MD-Simulations," *E. Phys. J. Web of Conferences* **15** (1–4), 03002 (2011).
14. A. E. Galashev and V. A. Polukhin, "Computer Study of Silver Absorption by Porous Silicon Dioxide Nanoparticles," *Kolloid. Zh.* **73** (6), 764–771 (2011).
15. V. A. Polukhin, E. D. Kurbanova, L. K. Rigmant, and N. A. Vatolin, "Thermal Stability of Ni and Pd Nanoclusters. MD Experiment," *Perspektivnye Materialy, Ser. Funktsional'nye Nanomaterialy, Vysokochistye Veshchestva*, 93–99 (2011).
16. A. V. Evteev, E. V. Kosilov, and E. A. Mikhailov, "Equilibrium Structure of Small Pd Clusters," in *Proceedings of VII International Conference on Solid-State Chemistry and Modern Micro- and Nanotechnology, Stavropol'* (SevKavGTU, Stavropol', 2009), pp. 70–72.
17. S. Ino, "Stability of Multiplay-Twinned Particles," *J. Phys. Soc. Japan* **27** (4), 941–953 (1969).
18. E. D. Kurbanova and V. A. Polukhin, "MD Simulation of Thermosize Effects and the Isomerization of Nickel and Palladium Nanoclusters," in *Proceedings of International Conference on Ultradispersed Powders, Nanostructures, and Materials: Production, Properties, Application, Krasnoyarsk* (Krasnoyarsk, Nauchn. Tsentr SO RAN, Krasnoyarsk, 2009), pp. 11–13.
19. K.-M. Choi, T. Mizugaki, K. Ebitani, and K. Kaneda, "Nanoscale Palladium Cluster Immobilized on a TiO<sub>2</sub> Surface as an Efficient Catalyst for Liquid-Phase Wacker Oxidation of Higher Terminal Olefins," *Chem. Lett.* **32** (2), 180–185 (2003).
20. E. D. Kurbanova, V. A. Polukhin, and A. E. Galashev, "Effect of the Character of Cluster/Substrate Interatomic Bonds on the Structure and Properties of 2D Spacers TM: Ni, Pd, Fe/Graphene (Quartz)," in *Proceedings of XIII All-Russia Conference on Structure and Properties of Metallic and Slag Melts, Yekaterinburg* (UrO RAN, Yekaterinburg, 2011), Vol. 1, pp. 30–33.
21. Daojian Cheng and Jianhui Lan, "Thermal Behavior of Pd Clusters inside Carbon Nanotubes: Insights into the Cluster-Size, Tube-Size, Metal-Tube Interaction Effects," *Molecular Simulation* **36**, 805–814 (2009).
22. A. T. N'Diaye, T. Gerber, C. Buss, et al., "A Versatile Fabrication Method for Cluster Superlattices," *New J. Physics* **11**, 1030451–1030459 (2009).
23. Zhiping Xu and J. Markus, "Buehler Interface Structure and Mechanics between Graphene and Metal Substrates: A First Principles Study," *J. Physics: Condensed Mater* **22**, 4853011–4853015 (2010).
24. Min Gao, Yi Pan, Chendong Zhang, et al., "Tunable Interfacial Properties of Epitaxial Graphene on Metal Substrates," *Applied Physics Letters* **96**, 0531091–0531096 (2010).
25. Y. L. Wang, A. A. Saranin, A. V. Zotov, et al., "Random and Order Arrays of Surface Magic Clusters," *International Reviews in Physical Chemistry* **27**, 317–360 (2008).